PERFORMANCE ASSESSMENT OF POSITIONING SOLUTIONS OF DIFFERENT MOBILE DEVICES USING KALMAN FILTERING

Inkaran Sivarasa[1], Jenan Rajavarathan[1], Guenther Retscher[2,*], Vipula Abeyratne[1],
Thilantha Lakmal Dammalage[3], Jelena Gabela[2], Vassilis Gikas[4]

[1] Faculty of Geomatics, Sabaragamuwa University of Sri Lanka (SUSL), Belihuloya, Sri Lanka;
s.inkaran@std.geo.sab.ac.lk, rjenan@geo.sab.ac.lk;
[2] Department of Geodesy and Geoinformation, TU Wien – Vienna University of Technology, Vienna, Austria;
guenther.retscher@tuwien.ac.at, jelena.gabela@geo.tuwien.ac.at;
[3] Estate and Built Environment, University of New England, Australia;
thilantha.dammalage@une.edu.au;
[4] School of Rural, Surveying and Geoinformatics Engineering, National Technical University of Athens, Greece;
vgikas@central.ntua.gr
[*] corresponding author: guenther.retscher@tuwien.ac.at

KEY WORDS: GNSS, Single-frequency GNSS, Dual-frequency GNSS, Kalman Filter, Performance analysis, Smartphone positioning.

ABSTRACT:

In this study, the performance of two different smart mobile devices is analysed and compared. These devices are either single-frequency or dual-frequency GNSS carrier frequency-enabled smartphones. Both selected devices are from the same manufacturer. They are the Pixel 3 and Pixel 4 from Google. The smartphones were positioned on six control points in an open sky environment for which ground truth was determined with high-precision geodetic GNSS equipment serving as a reference. For the evaluation, a Kalman filter solution is derived and applied to be able to determine position information epoch-wise. In the first step, the position solution variations on the control points are determined and analyzed. It is seen that high variations may occur, especially in the single-frequency Pixel 3 where high variations were shown. As expected, these deviations are significantly smaller for the dual-frequency Pixel 4. Using the Kalman filter it is then proven that positioning of the few decimeter to meter level is achievable for the dual frequency smartphone. Thus, it has been shown that dual-frequency smartphones have already reached a good level of performance which opens up their use for some applications in surveying and especially in Location-based Services (LBS).

1. INTRODUCTION

The Global Navigation Satellite System (GNSS) has emerged as one of the key tools widely used to determine positioning, navigation and timing (PNT) services and applications. The development of low-cost GNSS receivers has further improved their usage in common day-to-day applications. These receivers, which are incorporated into mobile devices, serve as a potential positioning tool for location-based service (LBS) applications. However, the PNT solutions derived on both the high-end and the low-cost GNSS receivers suffer from a well-known number of errors such as multipath, tropospheric and ionospheric delays, orbital errors and receiver noises. Comparatively, errors on these low-cost GNSS receivers are higher than on the geodetic grade devices mainly due to the utilization of low-cost antennas, multiplicative and additive noises (Huang et al., 2013, Paziewski et al., 2021). Further, mobile phones equipped with low-cost GNSS receivers and antennae and having low internal space, suffer extensively with larger Carrier-to-noise (C/N0) in comparison to geodetic receivers.

Sri Lanka being a developing country has been supported with technical development in geospatial sciences by a number of development projects, one of which is LBS2ITS, a European-Union funded project Erasmus + Capacity Building in Higher Education (Retscher et al., 2021) focusing on development in LBS and Intelligent Transport Systems (ITS) within the country. This work is one of the collaborative works of the project participants, performed to study and understand the comparative standalone GNSS positioning accuracies of single-frequency (SF) and dual-frequency (DF) mobile devices with respect to geodetic grade GNSS receivers. Further, we analysed the suitability of applying Kalman filtering on the static, standalone mobile GNSS observations for post-processing positional augmentations.

The paper is structured as follows: In section 2 the establishment of the control points and the set-up during the experiments for the GNSS performance tests with the smart mobile devices are presented. This is followed by section 2.3 where the use of a Kalman filter for data analysis of the smartphone observations on the control points is introduced for epoch-wise positioning. For this purpose, the main equations of the evaluation process are derived. Section 3 is the main part of the paper dealing with the analysis of the measurement campaign. Here in section 3.1 firstly the positioning variations of the observation data of the employed single (SF) and dual (DF) carrier frequency enabled smartphones in comparison to the ground truth and then the results of the Kalman filtering in section 3.2 are discussed in detail. For the Kalman filtering always the results before and after applying the filter are compared. Finally, some remarks and a summary of the main results conclude the paper.

2. FIELD EXPERIMENTS AND METHODOLOGY

2.1 Control Point Establishment and Static Observation

The study was designed with a focus on the collection of high-quality GNSS satellite observation data and mitigation of the external GNSS error factors. For the data collection, a combination of geodetic GNSS receivers and mobile phones with single and dual-frequency capabilities were employed. The Stonex S900A is a geodetic grade GNSS receiver with the capability of tracking multi-constellation GNSS satellites, i.e., from GPS, GLONASS, Galileo, and BeiDou. It was used as the primary device to provide a reference for the observation with the mobile devices. Six control points were established within the main ground of Sabaragamuwa University of Sri Lanka (SUSL) at corners of a rectangular shape, which were designed to minimize external disturbances for the reception of GNSS signals.

2.2 Mobile Phone GNSS Observations

For the performance analysis of mobile devices, four smartphones were used namely the Google Pixel 3, Pixel 4, Poco F3, and Xiaomi Redmi Note 8. The Pixel 4, Poco F3 and Redmi Note 8 mobile devices had capabilities to track dual-frequency GNSS observations (L1 and L5 frequencies in the case of GPS), while the Pixel 3 had capability to track single-frequency observations (L1 signal). Though the Redmi Note 8 device had the capability to track both, the L1 and L5 signals, it could track only the L1 frequency observations in the working scenario. Observations on the mobile devices were performed on a specially designed set-up over each point, facing the internal GNSS antenna towards the horizon as shown in Figure 1. Further, in order to reduce the ionospheric impact on the observations, the observation was performed during the nighttime, when the ionosphere over Sri Lanka is known to be quiet. The reference coordinates of each point were calculated through Precise Point Positioning (PPP) processing utilizing the survey grade GNSS observations.

Figure 1. Smartphone set-up over a control point.

2.3 Kalman Filter Derivation for Static Observations

A Kalman filter is an optimal estimator. It is recursive so that new measurements can be processed as they arrive. The aim of the Kalman filter process is to find the best estimate from the noisy observation data amounts while filtering out noise. In addition, the approach does not only clean up the measurements but also projects them onto the state estimate. A Kalman filter requires two models:

1. System model; and
2. Observation model.

The system model is given as:

$$\begin{aligned} x_n &= F_n x_{n-1} + w_n \\ w_n &\sim \mathcal{N}(0, Q_n). \end{aligned} \tag{1}$$

The state vector estimated at timestamp n is denoted by x_n and F_n denotes the transition matrix. w is the Gaussian process noise with zero mean and variance matrix Q. In this case, because GNSS receiver is static, the variance matrix is equal to zero as there is no movement.

The measurement model is given as

$$z_n = H_n x_n + v_n. \tag{2}$$

Vector z_n denotes the measurements at epoch n. H_n is the measurement matrix at time epoch n and it is a Jacobian matrix as it consists of the first-order partial derivatives of the non-linear measurement model. The measurement noise is denoted by v_n and it is assumed to be Gaussian with zero mean and variance matrix R.

Generally, the Kalman filter consists of two steps:

1. Time update (”prediction”) and
2. Measurement update (”correction”).

The first step, i.e., the time update (”prediction”), is done in the functional model as follows:

$$\hat{x}_n^- = F_n \hat{x}_{n-1}^+. \tag{3}$$

$\hat{x}_{n-1}^+$ denotes the state estimate from the previous epoch $n-1$. Symbol $+$ is used to denote the result of the correction step of the Kalman filter. $\hat{x}_n^-$ denotes the current, predicted, state estimate in epoch n. Symbol $-$ is used to denote the result of the prediction step of the Kalman filter. Like before, F_n is a transition matrix.

The variance-covariance matrix corresponding to the propagated state vector needs to be propagated as well. The following form is applied for the stochastic model

$$P_n^- = F_n P_{n-1}^+ F_n^T. \tag{4}$$

The predicted variance-covariance matrix is denoted with P_n^-. The corrected variance-covariance matrix from the previous epoch is denoted by P_{n-1}^+. The transpose matrix is denoted by $(\cdot)^T$. Normally, process noise would be added to the previous noise. However, as explained before, the process noise variance matrix Q is assumed to be zero.

https://doi.org/10.5194/isprs-archives-XLVIII-1-W1-2023-451-2023 | © Author(s) 2023. CC BY 4.0 License.

In the second step, the correction is performed based on the measurement update. Firstly, Kalman gain is calculated as shown in the following equation. It represents the weight given to the current measurements in order to update the state.

$$K_n = P_n^- H_n^T (H_n P_n^- H_n^T + R_n)^{-1} \tag{5}$$

where K denotes the Kalman Gain matrix estimate at epoch n. It is calculated based on the current measurement matrix H_n, predicted variance-covariance matrix P_n^- and measurement variance matrix R

The state update shown in Equation 6 is calculated based on the predicted state, Kalman gain, and the difference between the measurements z_n and the predicted measurements.

$$\hat{x}_n^+ = \hat{x}_n^- + K_n(z_n - H_n \hat{x}_n^-) \tag{6}$$

Finally, the variance-covariance matrix can be updated as:

$$P_n^+ = (I - K_n H_n) P_n^- (I - K_n H_n)^T + K_n R_n K_n^T. \tag{7}$$

These equations were processed in MATLAB. In the following section, the major results of this method are presented.

3. RESULTS AND ANALYSIS

The different capabilities of the devices used in the study impact the accuracy of the collected data, i.e., frequency and models of the mobile devices. The study accounted for these differences by calibrating the devices and applying appropriate processing techniques during data collection and analysis. Additionally, statistical methods to account for differences in the devices' capabilities were applied in the evaluation to estimate the uncertainty in the data collected. A Kalman filter as given in section 2.3 was used to estimate the positioning solutions for every epoch over the duration of the measurements. Confidence intervals for the measurements were then calculated to be able to analyse the achievable performance and positioning accuracies.

The use of multiple devices with different frequency capabilities allows for investigating the impact of the number of frequencies on GNSS positioning accuracy, particularly on mobile devices. By comparing the results obtained from the different devices, it is possible to evaluate the performance of consumer-grade GNSS receivers and assess the potential of using smartphones for GNSS data collection. Overall, it is important for studies like this to carefully consider the limitations of the equipment being used and to take appropriate steps to account for these limitations in data processing and analysis.

3.1 Positional variation of SF and DF mobile devices – Study over Point 9002 and 9003

The positional variation on North (N) and East (E) of a single-frequency (SF) (Pixel 3) and dual-frequency (DF) (Pixel 4) mobile devices are presented in Figure 2. This shows a better performance of the Pixel 4 mobile, which was further demonstrated through the calculations of Standard Deviation (STD) and Root Mean Square (RMS) values. The SD of the Pixel 4 mobile over Point 9002 was 4.46 m and 5.99 m in the N and E directions, respectively. For the Pixel 3, it was 14.79 m and 10.58 m in N and E directions, respectively. Further, the RMS error was comparatively high for the Pixel 3, which was 14.89 m and 10.72 m in N and E directions, respectively, and was around 5.14 m and 6.10 m for the Pixel 4 in N and E directions, respectively. A similar kind of performance of the Pixel 4 mobile could be noticed over all considered six reference points, with very minor deviations, which would be further discussed with satellite geometry and the surrounding environment in the extended study.

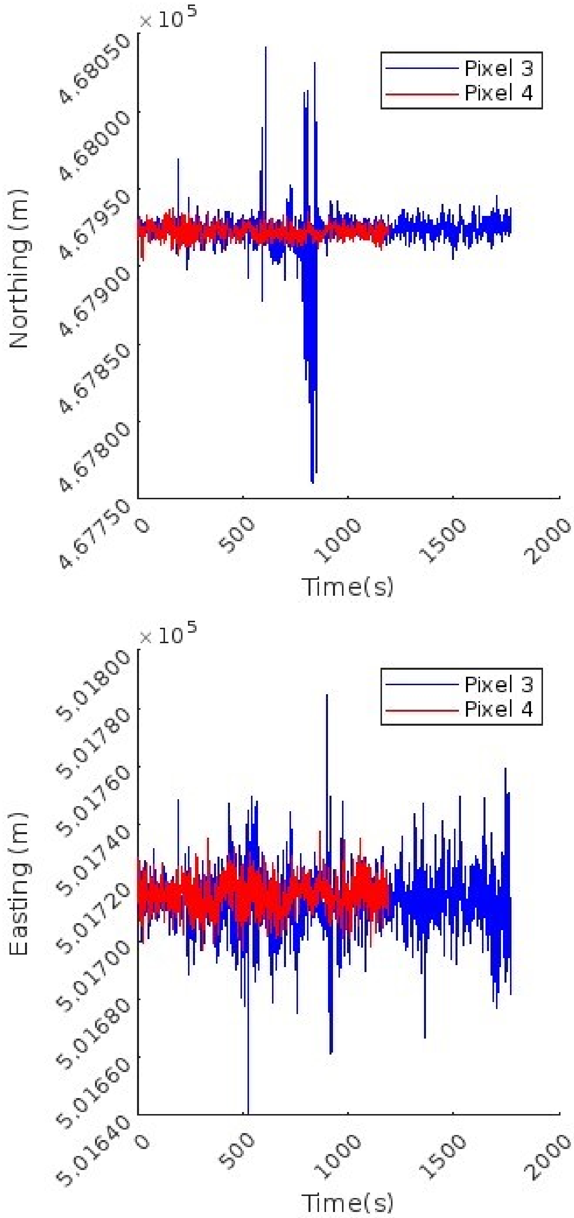

Figure 2. Positioning variation in N and E directions of the Pixel 3 (SF) and Pixel 4 (DF) over the Point 9002.

Due to the limited room in this paper, here just the results of a second point are presented here in Figure 3. The results on this point 9003 prove that the Pixel 4 performs better. The STD of the Pixel 4 mobile over point 9003 was 3.42 m and 4.76 m in the N and E directions, respectively, which was lower with the Pixel 3 of 7.21 m and 7.98 m in N and E directions, respectively. Further, the RMS error was comparatively high using the Pixel 3, which was 7.28 m and 8.33 m in N and E directions, respectively, and around 3.42 m and 4.81 m with the Pixel 4 in N and E directions, respectively.

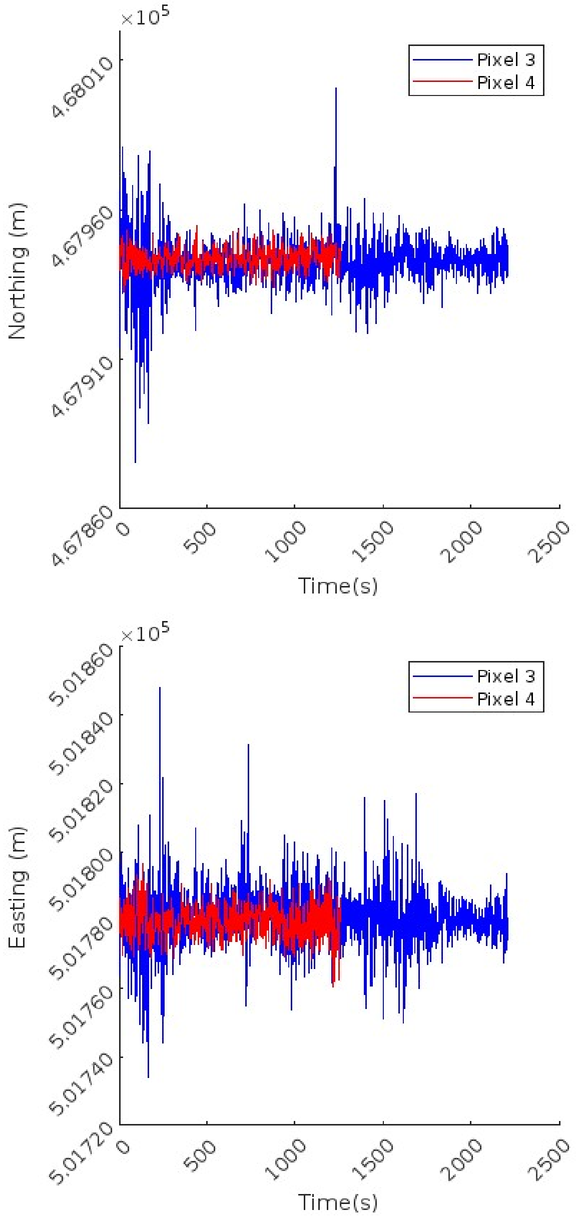

Figure 3. Positioning variation in N and E directions of the Pixel 3 (SF) and Pixel 4 (DF) over Point 9003.

3.2 Application of the Kalman filter on SF and DF mobile devices — Study over Point 9005

A Kalman filter for epoch-wise position estimation was applied on the SF and DF mobile GNSS observations, which produced an improvement in positional accuracies on both devices. As shown in Figure 4, the position deviations from the ground truth of the SF mobile (Pixel 3) were highly varying between ± 10 m in N and E directions with significant fluctuations and sudden outliers of more than ± 20 m, which have been made smoother with only minor variations with the application of the Kalman filter. The Kalman filter improved the RMS to 3.14 m and 3.59 m, from 9.00 m and 10.37 m in N and E directions, respectively. Further, a significant improvement could be seen for the deviations on the DF mobile device as well as it could be seen in Figure 5. The RMS of 3.55 m and 3.90 m in N and E directions was reduced to 1.23 m and 0.66 m after applying the Kalman filter on the GNSS raw measurements.

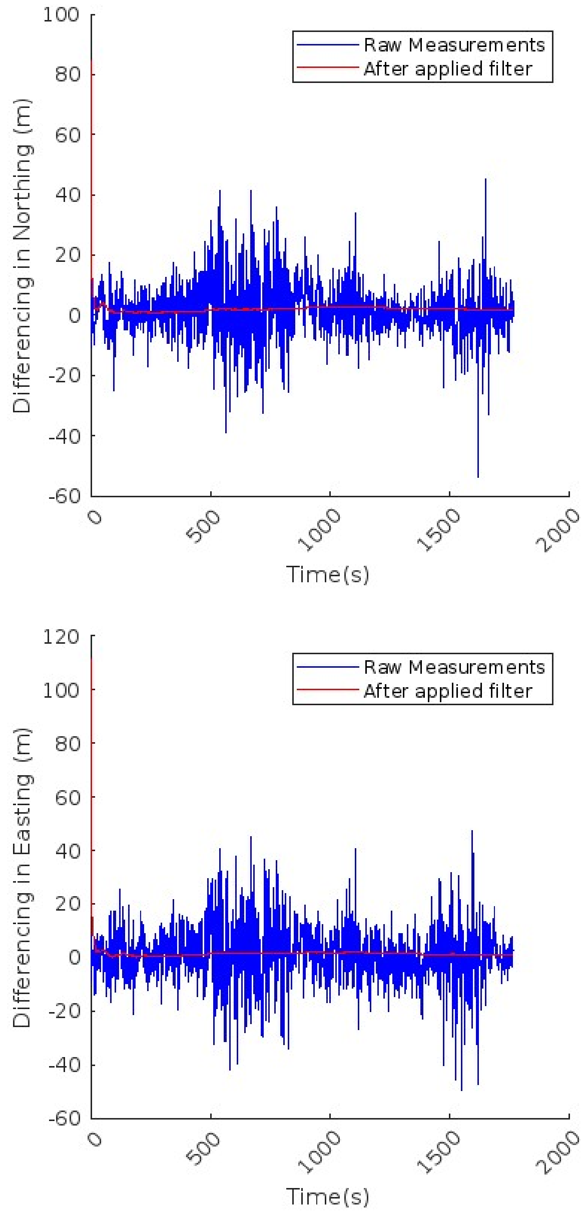

Figure 4. N and E deviations before and after applying a Kalman filter on the SF mobile (Pixel 3) over Point 9005.

For visualization of the position variations, scatter plots of the GNSS observations of the SF and DF mobile devices over Point 9005 were produced and are shown in Figure 6. The SF mobile (Pixel 3) observation shows a larger scattering of the raw GNSS measurements with no clear pattern. The position uncertainty is described by the size and orientation of the error ellipse (Jassim, 2019) with a length of the semi-major and -minor axes of around 30.87 m and 12.34 m, respectively. By using the Kalman filter it was reduced to 9.76 m and 0.68 m. Noticeable is the elongated shape of the error ellipses. The DF mobile (Pixel 4) observations show significantly lower scattering where the semi-major and -minor axes are comparatively smaller, around

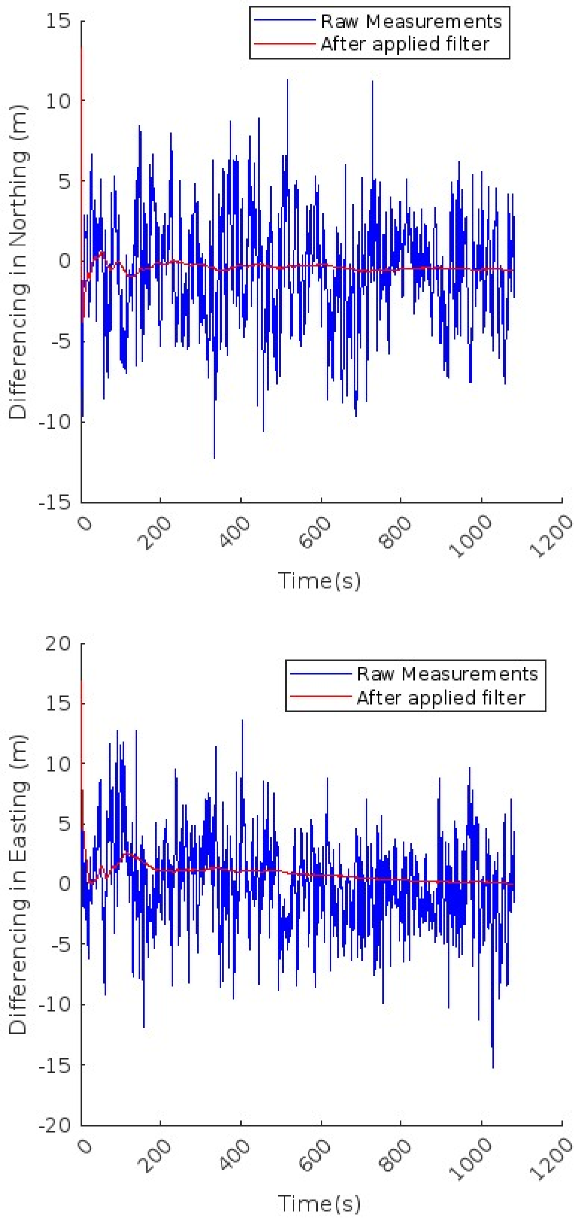

Figure 5. N and E deviations before and after applying a Kalman filter on the DF mobile (Pixel 4) over Point 9005.

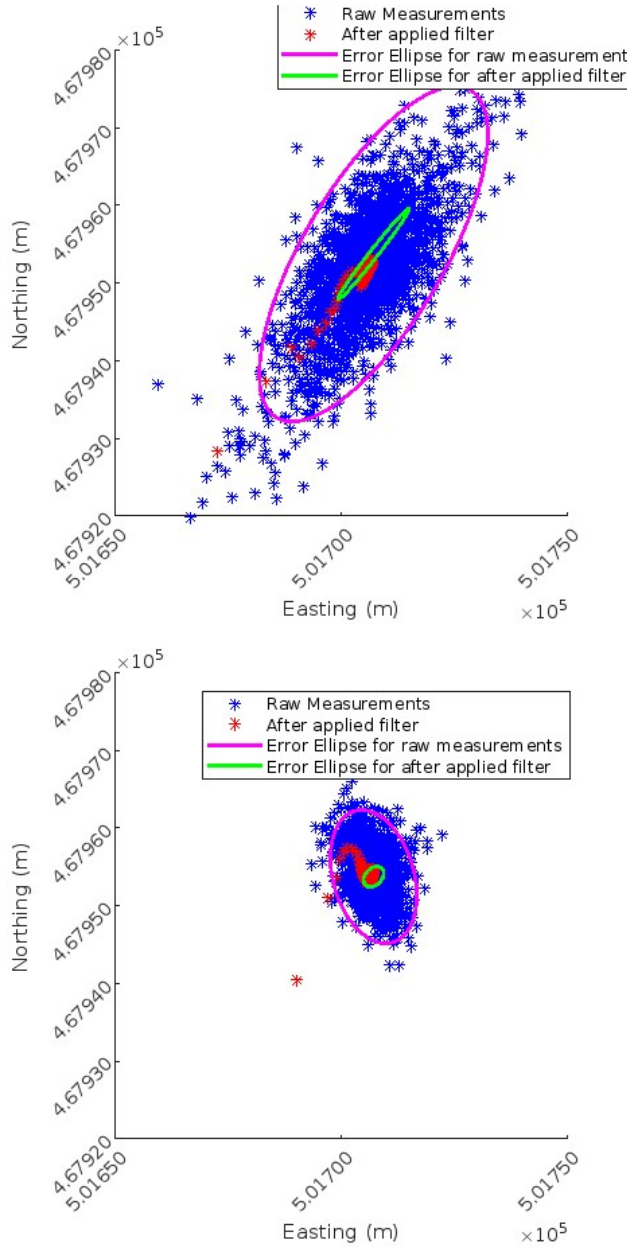

Figure 6. Scatter plots and error ellipses of the GNSS observations of the SF mobile (Pixel 3) on the top and the DF mobile (Pixel 4) on the bottom over Point 9005.

10.34 m and 7.62 m, respectively. These values were further reduced to around 2.28 m and 1.19 m when applying the Kalman filter. These results indicate that the use of a Kalman filter is practicable for epoch-wise positioning.

Figure 7 shows the predicted output position before and after applying the Kalman filter for Pixel 3 on the top and Pixel 4 on the bottom. The blue line represents the raw measurements before applying the Kalman filter calculated from the mean value for all six points, the red line represents the result after applying the filter and the green line represents the reference coordinates. The coordinates obtained before and after applying the Kalman filter indicate clearly the smaller differences from the reference coordinates for the Pixel 4. The Pixel 3, on the other hand, shows significant differences. This proves the previously presented results for all points in the rectangular shape selected.

Numerical values of the RMS are presented in Table 1 for three different control points. As can be seen, the application of the Kalman filter is able to significantly reduce the position deviations, especially in cases where the deviations are quite large. The worst performance of both the mobiles Pixel 3 and Pixel 4 is seen over Pt 9000 and Pt 9004, which is very well depicted alos in Figure 7. Pixel 3 has a very large RMS of deviation from the ground truth of 20.49 m. This can be reduced to 13.59 m when the Kalman filter is applied. Pixel 4 with an RMS of 7.61 m achieved 2.43 m when applying the filter.

4. CONCLUSIONS

The paper analyses the performance of the use of smart mobile devices in surveying. Tests are conducted in an open sky setting with single (SF) and dual (DF) carrier frequency-supported smartphones. For the study in this paper the results of the two

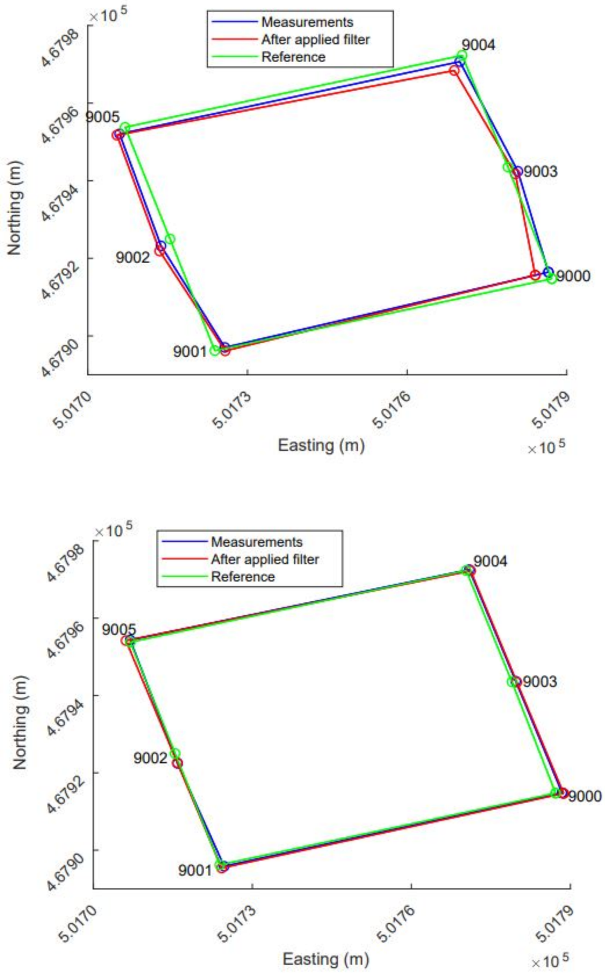

Figure 7. Positions of the points according to the average coordinates of Pixel 3 on the top and Pixel 4 on the bottom.

Mobile device	Pt 9000	Pt 9004	Pt 9003
Pixel 3	20.49	20.19	11.07
Pixel 3 KF applied	13.59	9.75	1.31
Pixel 4	7.61	6.83	5.90
Pixel 4 KF applied	2.43	2.02	3.17

Table 1. RMS values in [m] on three observation points before and after the application of Kalman Filter (KF).

smartphones Pixel 3 (SF) and Pixel 4 (DF) of the manufacturer Google are analyzed. In the first step, the positioning variations on six control points are analyzed. For these points, the ground truth was determined with a static survey using the geodetic GNSS equipment from the manufacturer Stonex, i.e. the Stonex S900 GNSS receiver. It is seen that the variations are quite high from the ground truth. As expected the DF smartphone, i.e., the Pixel 4, performs better. So it can be concluded from this first analysis that DF mobile devices perform well during static GNSS positioning. The performance of the SF mobile device was significantly lower.

In the next step the observation data is processed with a Kalman filter and compared to the results without applying filtering. A significant improvement while applying a Kalman filter in position estimation could be seen through this study. As expected, the application of the Kalman filter is more effective on the DF mobile device (Pixel 4) observations compared to that of the SF mobile device (Pixel 3). Scatter plots and resulting confidence ellipses were analyzed in detail for the observation on the control points where it was seen that the Kalman filter is capable to reduce the position deviations and noise significantly. Thus, it can be concluded that the obtained results indicate that the use of a Kalman filter is practicable for epoch-wise positioning. Then it is possible to achieve results on the few decimeter to meter level for the deviations from the ground truth.

In the extended future work we are studying the impact of the surrounding environment on the positioning accuracy of these two mobile devices. Furthermore, the performance of other different mobile devices will also be analyzed.

ACKNOWLEDGEMENT

The authors would like to acknowledge the passing of our dear colleague and co-author Vipula Abeyratne. We would like to dedicate this publication to Mr Abeyratne and express our gratitude for all the time we have spent together and all the work we have done together.

The authors acknowledge the funding for the project 618657-EPP-1-2020-1-AT-EPPKA2-CBHE-JP from the Erasmus+ Capacity Building in Higher Education programme. This project, with support from the European Commission, has funded the purchase of the Stonex S900 GNSS receiver used in this publication. This publication reflects the views only of the authors, and the Commission cannot be held responsible for any use which may be made of the information contained therein.

Co-funded by the
Erasmus+ Programme
of the European Union

REFERENCES

Huang, P., Pi, Y., Progri, I., 2013. GPS Signal Detection under Multiplicative and Additive Noise. *The Journal of Navigation*, 66(4), 479–500.

Jassim, A. M., 2019. The Ellipse of Position Error. *Zanco Journal of Pure and Applied Sciences*, 31(s3), 324-328. https://zankojournal.su.edu.krd/index.php/JPAS/article/view/3257.

Paziewski, J., Fortunato, M., Mazzoni, A., Odolinski, R., 2021. An analysis of multi-GNSS observations tracked by recent Android smartphones and smartphone-only relative positioning results. *Measurement*, 175, 109162. https://www.sciencedirect.com/science/article/pii/S0263224121001858.

Retscher, G., Gikas, V., Gerike, R., 2021. Curricula enrichment for sri lankan universities delivered through the application of location-based services to intelligent transport systems. *FIG eWorking Week 2021*.